Human Brain Mapping

WILEY

RESEARCH ARTICLE OPEN ACCESS

Real-Time Tractography-Assisted Neuronavigation for Transcranial Magnetic Stimulation

Dogu Baran Aydogan[1,2,3] | Victor H. Souza[2,3,4] | Renan H. Matsuda[2,5] | Pantelis Lioumis[2,3,6] | Risto J. Ilmoniemi[2]

[1]A.I. Virtanen Institute for Molecular Sciences, University of Eastern Finland, Kuopio, Finland | [2]Department of Neuroscience and Biomedical Engineering, School of Science, Aalto University, Espoo, Finland | [3]Aalto NeuroImaging, School of Science, Aalto University, Espoo, Finland | [4]Graduate Program in Rehabilitation Sciences and Functional Physical Performance, School of Physiotherapy, Federal University of Juiz de Fora, Juiz de Fora, Brazil | [5]Department of Physics, School of Philosophy, Science and Letters at Ribeirão Preto, University of São Paulo, Ribeirão Preto, Brazil | [6]BioMag Laboratory, HUS Medical Imaging Center, University of Helsinki, Helsinki University Hospital and Aalto University, Helsinki, Finland

Correspondence: Dogu Baran Aydogan (baran.aydogan@uef.fi)

Received: 18 April 2024 | **Revised:** 29 November 2024 | **Accepted:** 15 December 2024

Funding: This work was supported by Research, Innovation and Dissemination Center for Neuromathematics, 2013/07699-0, Conselho Nacional de Desenvolvimento Científico e Tecnológico, 141056/2018-5, Academy of Finland, 348631, 349985, 353798, European Research Council, 810377, Helsingin ja Uudenmaan Sairaanhoitopiiri, TYH2022224.

Keywords: brain stimulation | connectivity | diffusion MRI | neuronavigation | TMS | tractography

ABSTRACT

State-of-the-art navigated transcranial magnetic stimulation (nTMS) systems can display the TMS coil position relative to the structural magnetic resonance image (MRI) of the subject's brain and calculate the induced electric field. However, the local effect of TMS propagates via the white-matter network to different areas of the brain, and currently there is no commercial or research neuronavigation system that can highlight in real time the brain's structural connections during TMS. This lack of real-time visualization may overlook critical inter-individual differences in brain connectivity and does not provide the opportunity to target brain networks. In contrast, real-time tractography enables on-the-fly parameter tuning and detailed exploration of connections, which is computationally inefficient and limited with offline methods. To target structural brain connections, particularly in network-based treatments like major depressive disorder, a real-time tractography-based neuronavigation solution is needed to account for each individual's unique brain connectivity. The objective of this work is to develop a real-time tractography-assisted TMS neuronavigation system and investigate its feasibility. We propose a modular framework that seamlessly integrates offline (preparatory) analysis of diffusion MRI data with online (real-time) probabilistic tractography using the parallel transport approach. For tractography and neuronavigation, we combine our open source software Trekker and InVesalius, respectively. We evaluate our system using synthetic data and MRI scans of four healthy volunteers obtained using a multi-shell high-angular resolution diffusion imaging protocol. The feasibility of our online approach is assessed by studying four major TMS targets via comparing streamline count and overlap against offline tractography results based on filtering of one hundred million streamlines. Our development of a real-time tractography-assisted TMS neuronavigation system showcases advanced tractography techniques, with interactive parameter tuning and real-time visualization of thousands of streamlines via an innovative uncertainty visualization method. Our analysis reveals considerable variability among subjects and TMS targets in the streamline count, for example, while 15,000 streamlines were observed for the TMS target on the visual cortex (V1) of subject #4, in the case of subject #3's V1, no streamlines were obtained. Overlap analysis against offline tractograms demonstrated that real-time tractography can quickly cover a substantial part of the target areas' connectivity, often surpassing the coverage of offline approaches within seconds. For instance, significant portions of Broca's area and the primary motor cortex were effectively visualized after

generating tens of thousands of streamlines, highlighting the system's efficiency and feasibility in capturing brain connectivity in real-time. Overall, our work shows that real-time tractography-assisted TMS neuronavigation is feasible. With our system, it is possible to target specific brain regions based on their structural connectivity, and to aim for the fiber tracts that make up the brain's networks. Real-time tractography provides new opportunities for TMS targeting through novel visualization techniques without compromising structural connectivity estimates when compared to the offline approach.

1 | Introduction

Transcranial magnetic stimulation (TMS) is a non-invasive brain stimulation technique approved in many countries for treating, for example, major depression disorder (MDD) (Fitzgerald et al. 2009) or obsessive-compulsive disorder (OCD) (Pelissolo et al. 2016), and for performing motor and speech cortical mapping as part of presurgical evaluation (Lefaucheur and Picht 2016; Krieg et al. 2017). The navigated TMS (nTMS) approach is also widely used to investigate brain functions by evoking motor or behavioral responses or by interrupting task-related processes (Grosprêtre, Ruffino, and Lebon 2016; Di Lazzaro and Rothwell 2014; Lefaucheur et al. 2014; Tremblay et al. 2019). However, defining optimal targets for TMS remains challenging, which is mostly done based on brain's morphology, using coordinates from atlases, or pre-defined locations from functional neuroimages, although state-of-the-art approaches also consider the induced electric field (E-field) strength at the target and surrounding (off-target) regions (Cash et al. 2021).

With a stimulation coil placed on the scalp, TMS induces a brief electric field that activates neurons in a limited range, depending on the stimulation intensity (Terao and Ugawa 2002). The precision of TMS interventions rely on accurately targeting the E-field to the desired cortical region, which is enabled via real-time visualization of the E-field distribution on the individual's brain anatomy obtained using structural MRI scans (Ruohonen and Karhu 2010; Hannula and Ilmoniemi 2017). While the advancements towards the incorporation of individual's unique cortical geometries for E-field computation are pivotal in helping maximize therapeutic efficacy (Dannhauer et al. 2024) the localized activation, however, propagates to different areas via the white-matter network (Van Essen 2013). Knowing which networks or connections of the brain are affected by TMS is important because structural connectivity of the brain plays a role in understanding and treating many brain disorders including MDD (Korgaonkar et al. 2014), Alzheimer's disease (Lo et al. 2010), multiple sclerosis (Llufriu et al. 2017) and stroke (Yamada et al. 2004). Connections in the brain's white matter can be detected non-invasively and in vivo with fiber tracking, that is, tractography, using diffusion magnetic resonance imaging (dMRI) (Shi and Toga 2017). During the last years, research based on tractography has contributed substantially to elucidating the circuitry of the human brain (Wandell 2016). Tractography can be performed on the whole brain, providing the structural connectome to study its network properties (Rubinov and Sporns 2010), or on selected, that is, seed, regions in the brain.

State-of-the-art nTMS systems provide real-time coil position and E-field estimate overlaid on the individual's structural T1-weighted MRI. The addition of real-time tractography information to the already existing nTMS would be highly valuable by enabling targeting of fiber tracts or regions that are remotely connected to the area under the coil. This enhancement is especially relevant for conditions where treatment outcomes depends not only on the stimulation of specific cortical regions but also on modulating the activity of networks where these regions are part of. For example, in treating disorders like MDD, where structural connections have been shown to be affected (Bracht, Linden, and Keedwell 2015; Korgaonkar et al. 2011), a tractography-assisted targeting approach could enhance the efficacy of TMS by guiding the operators to target the individual's desired structural network. Additionally, real-time tractography enables novel strategies to be employed for TMS-based cortical mapping that aims to localize brain regions responsible for certain functions like motor control, language, or sensory processing—a technique used for surgical planning (Krieg et al. 2017). Since TMS-induced responses are unknown prior to these experiments, real-time adjustments to coil positioning are essential. Real-time tractography provides crucial connectivity information about the TMS-affected areas, supporting dynamic decision-making for placing the coil. Specifically, during speech cortical mapping (Lioumis et al. 2012, 2023), if a naming error occurs due to TMS at a cortical site, operators can leverage real-time tractography to visualize how this site is connected to remote brain regions. This allows for the exploration of distant areas involved in speech function, prompting further investigation into regions that might otherwise be overlooked, thereby potentially enhancing the precision of consequent interventions. Similarly, real-time tractography offers new opportunities when performing TMS–EEG and paired associative stimulation (PAS) experiments, where predefining targets, using scalp-based coil placements or off-line tractography might be ineffective. During the actual experiment, these targets may cause muscle pain, artifacts, and discomfort, leading to poor measurements or even termination of the experiment, necessitating real-time adjustments. Additionally, these cortical sites may not produce relevant or strong enough responses, or may not perturb or engage the desired network, which can be improved by adjusting the coil placement based on real-time tractography.

However, introducing real-time structural connectivity estimation to existing nTMS systems is challenging. This is mainly due to the inherent limitations of tractography, which have been increasingly pointed out by validation studies (Thomas et al. 2014; Yendiki et al. 2022) and benchmarks through international tractography challenges (Maier-Hein et al. 2017; Nath et al. 2020; Schilling et al. 2021; Maffei et al. 2022). Importantly, tractography is well-known to miss connections that are present in the brain, that is, false negatives (Aydogan et al. 2018), and at the same time, it generates connections that do not exist, that is, false positives (Schilling et al. 2019).

The goal of this work was to develop a system that computes and displays the brain's structural connections in real time for guiding TMS. By leveraging real-time tractography, we aim to extend the focus of current nTMS systems beyond localized stimulation to take into account a more comprehensive understanding of the brain's interconnected networks. This approach enables us to inform our TMS targeting with insights into the interconnected networks of the brain, offering more comprehensive options for stimulation.

2 | Method

Figure 1 shows the overall workflow for the proposed real-time tractography-assisted TMS neuronavigation system. Our approach is based on a modular framework that seamlessly integrates the output from offline (preparatory) analysis with online (real-time) tractography and visualization. There is a clear separation between these two main components; the output of the offline part is not modified during real-time operation and is fed as input to the online part. We next explain the building blocks of the proposed approach, followed by our experiments on four healthy volunteers.

2.1 | Offline Processing

dMRI was preprocessed using Marcenko-Pastur PCA denoising algorithm (Veraart et al. 2016; Garyfallidis et al. 2014), and corrected for eddy-current and motion artifacts (Andersson and Sotiropoulos 2016). Due to partial-Fourier acquisition and scaling of diffusion-weighted images with the $b0$ image during compartment modeling, Gibbs artifacts and bias-field inhomogeneities were not removed. Fiber orientation distribution (FOD) image was computed using the compartment model approach in Tran and Shi (2015). For anatomically constrained tractography (Smith et al. 2012), labels for white matter, cerebrospinal fluid (CSF), and the region outside the brain were defined from Freesurfer's *reconall* (Fischl 2012). FOD was registered on the T1 space by computing the anisotropic power (Chen et al. 2019) and applying a rigid transform obtained with ANTs (Avants, Tustison, and Song 2009). Offline processing was completed with a visual quality inspection.

2.2 | Online Processing

2.2.1 | Tractography

2.2.1.1 | Fiber Tracking. Our parallel transport tractography (PTT) algorithm applies principles of differential geometry to generate smooth (C^1-continuous) streamlines. Unlike most algorithms that rely only on local measurements, PTT models a topographically organized (cylindrical) fiber bundle during propagation, and leverages regional FOD information, improving fiber tracking in complex white matter profiles (Aydogan and Shi 2019, 2021). PTT is implemented in our in-house developed, open-source software Trekker (https://dmritrekker.github.io/).

To reduce false positives, following anatomical constraints are applied:

1. To prevent improper termination→*discard_if_ends_inside* white matter
2. To prevent projecting through CSF→*discard_if_enters* CSF
3. To prevent leaking outside the brain→*stop_at_entry* outside the brain

2.2.1.2 | Visualization of Uncertainty. In this work, we introduce a novel visualization approach using

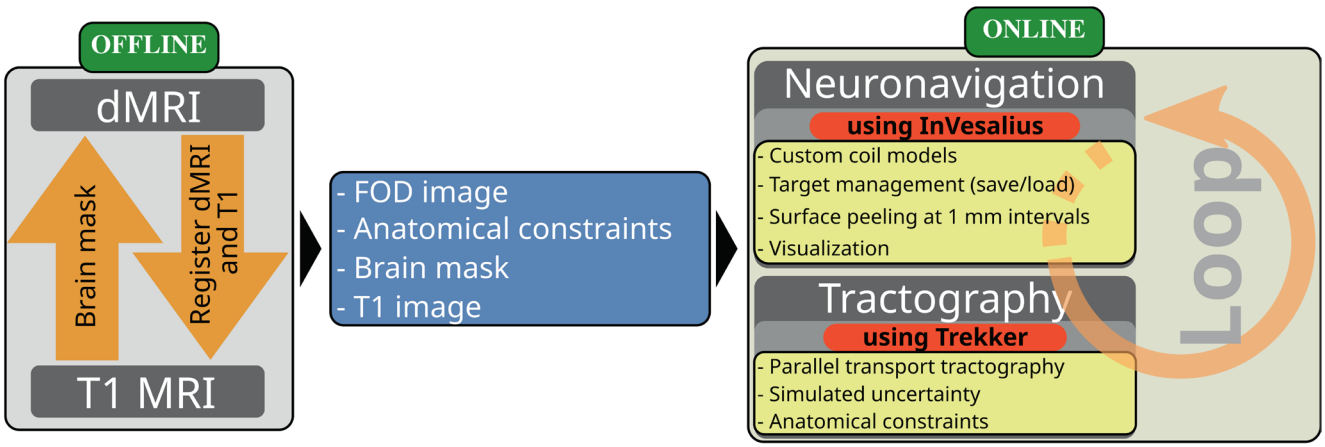

FIGURE 1 | For real-time tractography-assisted neuronavigation, we combine information from T1 and dMRI data. In the offline (preparatory) part, necessary inputs for the online (real-time) part are prepared. The necessary inputs are: (i) fiber orientation distribution (FOD) image, needed for fiber tracking, (ii) anatomical constraints, needed to reduce false positives during tractography by preventing improper termination within white matter and crossing through cerebrospinal fluid, (iii) segmented brain mask, needed to compute the peeled brain surfaces, and (iv) T1 image, to show the grayscale brain image on the peeled surfaces. The online part consists of the neuronavigation and tractography modules that continuously run in a multi-threaded loop. Neuronavigation and tractography are done using our custom software InVesalius (Souza et al. 2018) and Trekker (https://dmritrekker.github.io/), respectively. The main features used during real-time operation are inside the yellow boxes.

the observations in Aydogan et al. (2018), which reports performance trends in tractography based on parameter combination choices. For example, a low FOD threshold helps to find intricate connections, reducing false negatives, but at the same time this increases false positive streamlines. This known trade-off between sensitivity and specificity offers an opportunity to visualize uncertainty based on parameter choices. To visualize uncertainty, as shown in Figure 2, we designed a transfer function, which assigns each streamline an opacity value based on the fiber tracking parameter used to obtain that streamline, as initially introduced in Aydogan (2020).

2.2.2 | Implementation of Real-Time Tractography During Neuronavigation

The real-time visualization of tractograms was achieved by integrating Trekker in the open-source, free neuronavigation software InVesalius Navigator (Souza et al. 2018) (https://invesalius.github.io/). Tracking parameters are saved in a .json formatted text file, which can be modified using a text editor for instant manual adjustments. This provides the option for a more thorough exploration of connections, for example, by increasing the number of trials per seed point or using smaller curvature

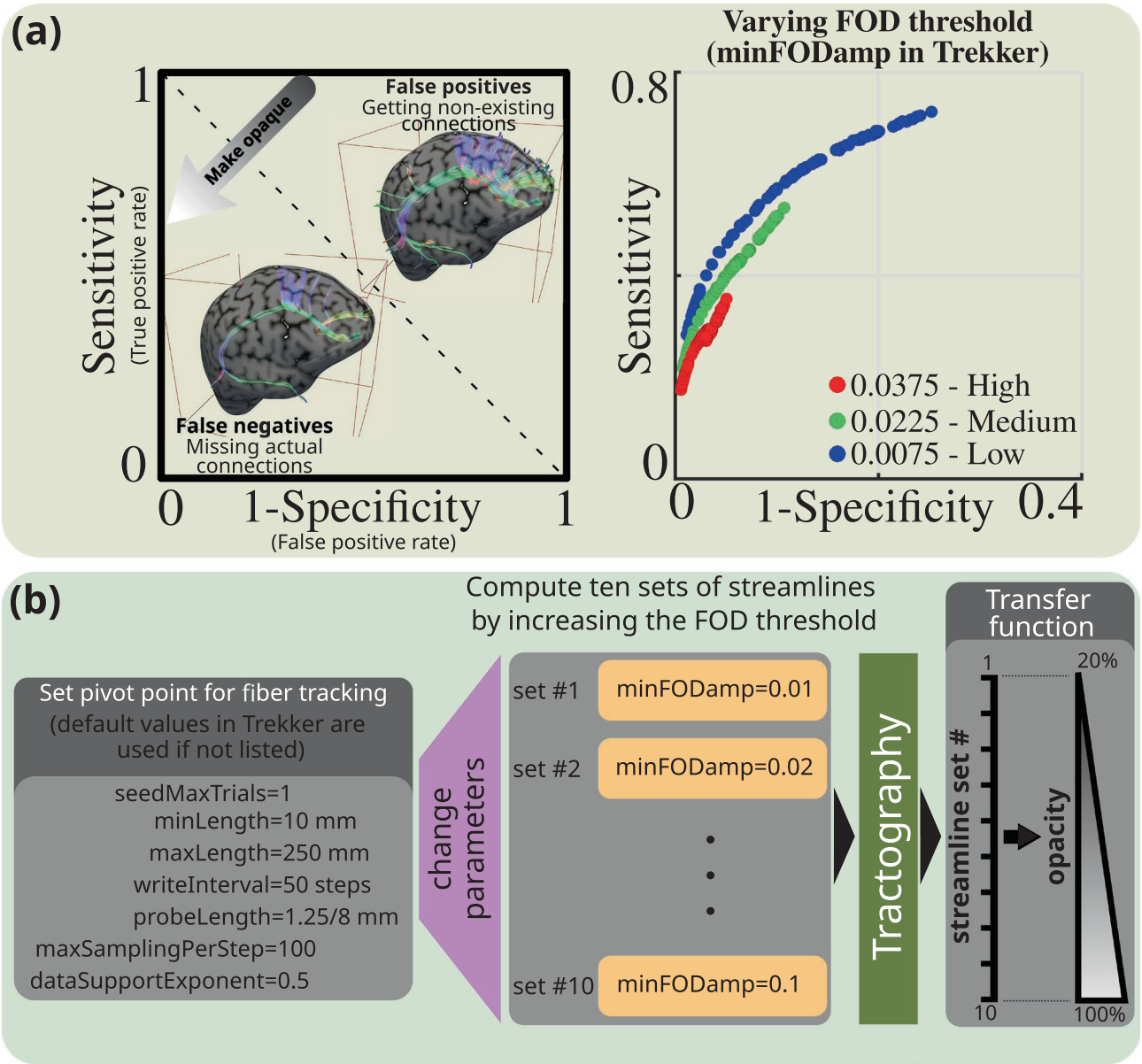

FIGURE 2 | (a) Sensitivity and specificity values based on voxel-wise overlap between dMRI-based tractography and ex vivo tracer injection experiments demonstrate the trade-off in tractography performance for various step size and curvature threshold combinations (81 samples) for each fixed FOD threshold value (Aydogan and Shi 2018). The ROC curve can be traversed by varying the FOD threshold (*minFODamp* parameter in Trekker). Low values for FOD threshold lead to increased sensitivity at the cost of decreased specificity. By displaying the streamlines generated using low FOD thresholds with more transparency, we provide visual information to the operator regarding increased possibility of false connectivity as a result of the corresponding parameter choice. (b) Fixed parameters used for fiber tracking and the range of values for the varying FOD threshold. The transfer function linearly maps the increasing FOD threshold to opacity values ranging from 20% to 100%.

thresholds for fiber tracking. During neuronavigation, a continuous loop starts when the tracking camera detects the TMS coil. Then, N seed coordinates for computing the streamlines are pseudo-randomly sampled inside a sphere with 1.5-mm radius, where N corresponds to the number of processor threads available on the computer. Each seed coordinate initiates the computation of one streamline. Thus, the larger the number of available processor threads, the more streamlines can be computed in parallel. The center of the sphere is defined as the point in the white matter with the smallest Euclidean distance to the central, longitudinal axis of a $2\times2\times20$-mm^3 rectangular prism grid. Grid points within the prism are spaced by 1 mm, and the points in the white matter are identified using the Freesurfer segmentation. The prism is oriented with its central, longitudinal axis along a line projected from the TMS coil center and offset by 30 mm from the coil surface. The offset was defined manually based on visual inspections from 15 MRIs to minimize the number of points of the prism in areas above the white matter, such as outside the head and on the scalp, skull, and CSF. At each iteration, the *minFODamp* parameter is adjusted as shown in Figure 2 and streamlines are visualized every 100 ms with the corresponding opacity. Because 10 parameter combinations are used for uncertainty visualization, these combinations are repeated at every 10th iteration. The loop runs continuously until 1000 streamlines are displayed or the coil is moved by at least 2 mm. This distance threshold avoids excessive removal and addition of streamlines for small jitters in the TMS coil coordinates. If the TMS coil moves more than 2 mm from the first point that the white matter was detected, streamlines that were previously displayed are removed; otherwise, they are continuously added.

3 | Experimental Setup

3.1 | Synthetic Characterization

We studied uncertainty visualization tracking parameters with offline experiments on the ISMRM 2015 tractography challenge dataset (http://www.tractometer.org/ismrm_2015_challenge/data) (Maier-Hein et al. 2017). We used the fiber tracking parameters shown in Figure 2 to compute 10 million streamlines in the whole brain by randomly seeding the white-matter mask. The process is repeated for each of the 10 *minFODamp* values. For studying the performance, bundle overlap and overreach were computed using the evaluation code available at https://tractometer.org/ismrm2015/tools/. These measures were used in the original challenge, allowing us to compare our results with the original submissions. For a given ground truth tractogram A and an evaluated tractogram B, overlap is defined as $|(B\cap A)|\ /\ |A|$, and overreach as $|(B\setminus A)|\ /\ |A|$. Here, $|.|$ represents the volume of regions, approximated by the number of the non-zero voxels in the discretized masks of traced voxels with streamlines, with each voxel having an isotropic dimension of $1\times1\times1$ mm^3.

3.2 | TMS Experiment

Experiments were done on four healthy male volunteers (age: 30–42) after collecting written informed consents. The study was done in accordance with the Declaration of Helsinki and approved by the Coordinating Ethics Committee of the Hospital District of Helsinki and Uusimaa.

3.2.1 | MRI Data

MRI measurements were done at the Advanced Magnetic Imaging Centre of Aalto NeuroImaging using a MAGNETOM Skyra 3T MR scanner (Siemens Healthcare, Erlangen, Germany) with a 32-channel head coil. For T1 image, a sagittal MPRAGE protocol with TE = 3.3 ms, TR = 2530 ms, $1\times1\times1$ mm^3 voxel dimension and $176\times256\times256$ voxels were used. The dMRI were acquired according to a multi-shell high-angular resolution diffusion imaging (HARDI) scheme with TE = 107 ms, TR = 3.9 s, $2\times2\times2$ mm^3 voxel dimension and $176\times256\times256$ voxels. Data were collected from 100 directions uniformly distributed on a sphere. A total of 18, 32, and 50 volumes were distributed to three shells with b-values 900, 1600, and 2500 s/mm^2, respectively. Eleven $b0$ images were interleaved in-between, and four reverse phase-encoded $b0$ images were collected for motion and distortion correction.

3.2.2 | TMS Experimental Protocol

Figure 3 shows our setup. Navigation was performed with an infrared Polaris Vicra camera (Northern Digital Inc., Waterloo, ON, Canada) and tracking probes with passive reflective spherical markers. Fiducial registration errors were kept below 3 mm (Souza et al. 2018). Experiments were performed with a Dell Precision 7530 (CPU Intel 6 core 2.6 GHz i7-8850H, 32 GB RAM, 1 TB SSD hard drive, NVidia Quadro P2000 graphics card, and Windows 10 64 bits).

We studied the feasibility of reliable and repeatable targeting of four major connections in the left hemisphere of the brain involved in: motor, cognitive, speech, and visual functions. Therefore, we targeted the (i) primary motor cortex (M1), (ii)

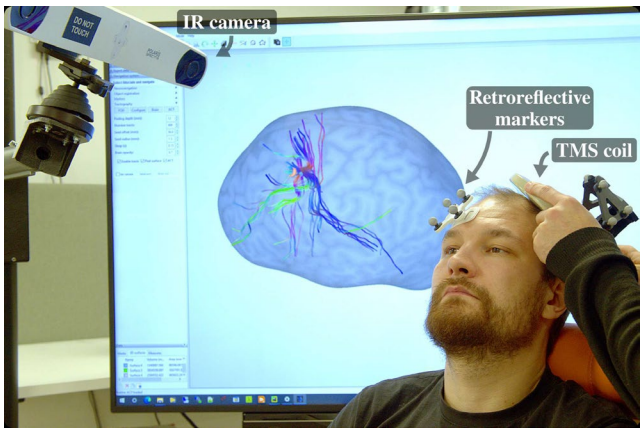

FIGURE 3 | Tractography-assisted nTMS setup. The display with the InVesalius user interface shows the peeled brain surface and the streamlines obtained from the real-time TMS coil position. The coil is being held by the operator and tracked by the neuronavigation software that analyzes data from an infrared (IR) camera and retroreflective markers.

dorsolateral prefrontal cortex (DLPFC), (iii) Broca's area (BA44), and (iv) primary visual cortex (V1), respectively. We initially saved the intended TMS target locations related to these four regions in the InVesalius software interface to guide the TMS coil placement. The M1 target was identified based on abductor pollicis brevis (APB) muscle twitches. DLPFC was identified visually from T1 MRIs as described in Lioumis et al. (2009). Broca's area was identified as described in speech cortical mapping studies (Lioumis et al. 2012; Corina et al. 2010; Krieg et al. 2017). The primary visual cortex was selected based on visual inspection of the anatomical MRIs and by applying single TMS pulses that elicited phosphenes in the participant's visual field.

For assessing the reproducibility of the displayed streamlines, we placed the TMS coil on the selected target and recorded the TMS coil coordinates and corresponding seed coordinates used to compute the streamlines in real time. This process was repeated 10 times for each of the four targets by removing the coil from the vicinity of participants' head after each trial.

3.2.3 | Data Analysis

We studied: (1) how offline filtering (selection) of streamlines compare against real-time tractography, and (2) the number of streamlines to display.

For (1), we generated 10 million streamlines for each of the 10 *minFODamp* values by randomly seeding the whole brain. Each tractogram was then filtered so that only those streamlines that passed through the 1.5-mm sphere centered at the recorded target points remained. For each target region, we reported the number of selected streamlines.

For (2), we investigated the overlap between the tractograms with increasing number of streamlines. For that, we first generated 100,000 streamlines from each seed using each of the 10 *minFODamp* values. The combined tractogram with 1 million streamlines was used as a reference. We then simulated the case during the real-time experiment, where only a subset of these streamlines were shown. To that end, we generated 7 subsets with 100, 300, 1000, 3000, 10,000, 30,000, and 100,000 streamlines. Each subset contained an equal number of streamlines computed with different *minFODamp* values. The overlap was computed using in-house code as $|(S \cap R)|/|R|$, consistent with the ISMRM 2015 challenge. Here S and R denote the subset and reference tractograms, respectively. Traced masks of streamlines, mapped on each subject's T1 image space, were obtained using thresholded (>0) track-density images (TDI) (Calamante et al. 2010) to approximate the covered volumes by counting the number of non-zero voxels.

4 | Results

4.1 | Synthetic Characterization

Figure 4 shows the overlap and overreach values relative to *minFODamp*, which is the parameter varied for uncertainty visualization. Overlap indicates tractogram alignment with the

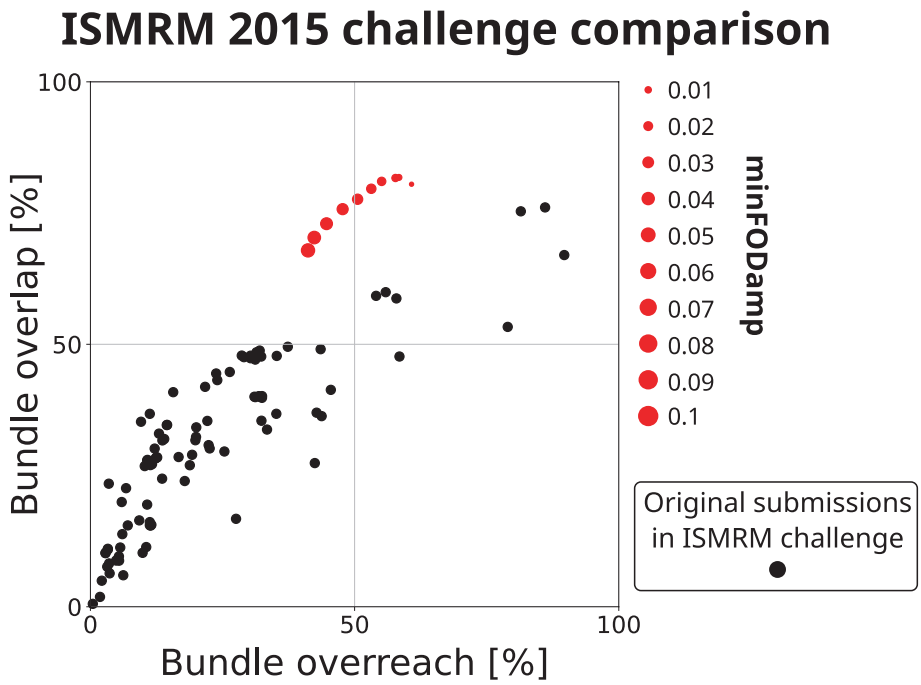

FIGURE 4 | The variation in tractography performance with respect to the changes in *minFODamp* parameter for uncertainty visualization was tested using the ISMRM 2015 tractography challenge data. Each red dot represents a score obtained for a tractogram with 10 million streamlines generated by randomly seeding the whole-brain mask using each of the 10 *minFODamp* parameters shown in Figure 2. The obtained scores with Trekker are highly competitive against the original submissions to the challenge. The trend shows the expected trade-off between true and false positives, where increasing the *minFODamp* parameter decreases bundle overreach, that is, false positives, at the cost of reduced bundle overlap, that is, true positives.

ground truth, that is, relates to true positives, while overreach shows how much of it extends beyond the ground truth, that is, relates to false positives.

To demonstrate the effect of uncertainty visualization in displaying structural connectivity, in Figure 5, we picked three tractograms that contain the cortico-spinal-tract (CST) and transcallosal connections through the corpus callosum (CC), which are both involved with motor functions commonly studied with TMS (Sollmann et al. 2020; Voineskos et al. 2010). Tractograms are then combined with and without uncertainty visualization. The three tractograms were obtained from whole-brain tractograms computed with *minFODamp* values of 0.01, 0.05, and 0.1, by selecting 500 streamlines within a sphere of radius 1.5-mm that was manually placed in the primary motor cortex.

4.2 | Navigated TMS With Real-Time Tractography

Our setup is shown in the Video S1. The operator can observe the structural connections while the coil is moved. For demonstrative purposes, the operator shows the connections on various locations. Consent of the model is obtained to publish his face in the Video S1.

4.3 | TMS Experiment

We compared the number of streamlines and overlap percentages using tractograms obtained offline. Figure 6 shows the number of streamlines obtained by filtering offline computed, large-scale whole-brain tractograms that contain 100 million streamlines for each subject. We observe that there is large variability among subjects, brain regions, and repetitions. Nearly 15,000 streamlines were obtained for many repetitions in the V1 area of subject #4. However, for the same area of subject #3, many times it was not possible to obtain any streamline. We observe a general trend of decreasing number of streamlines with the increase in *minFODamp*. For a few seed points, however, the number of streamlines increase with *minFODamp*, for example, M1 seed #4 of subject #2, highlighting the complex relationship between tractography parameters, connectivity profiles of the seed regions, and the individual variability.

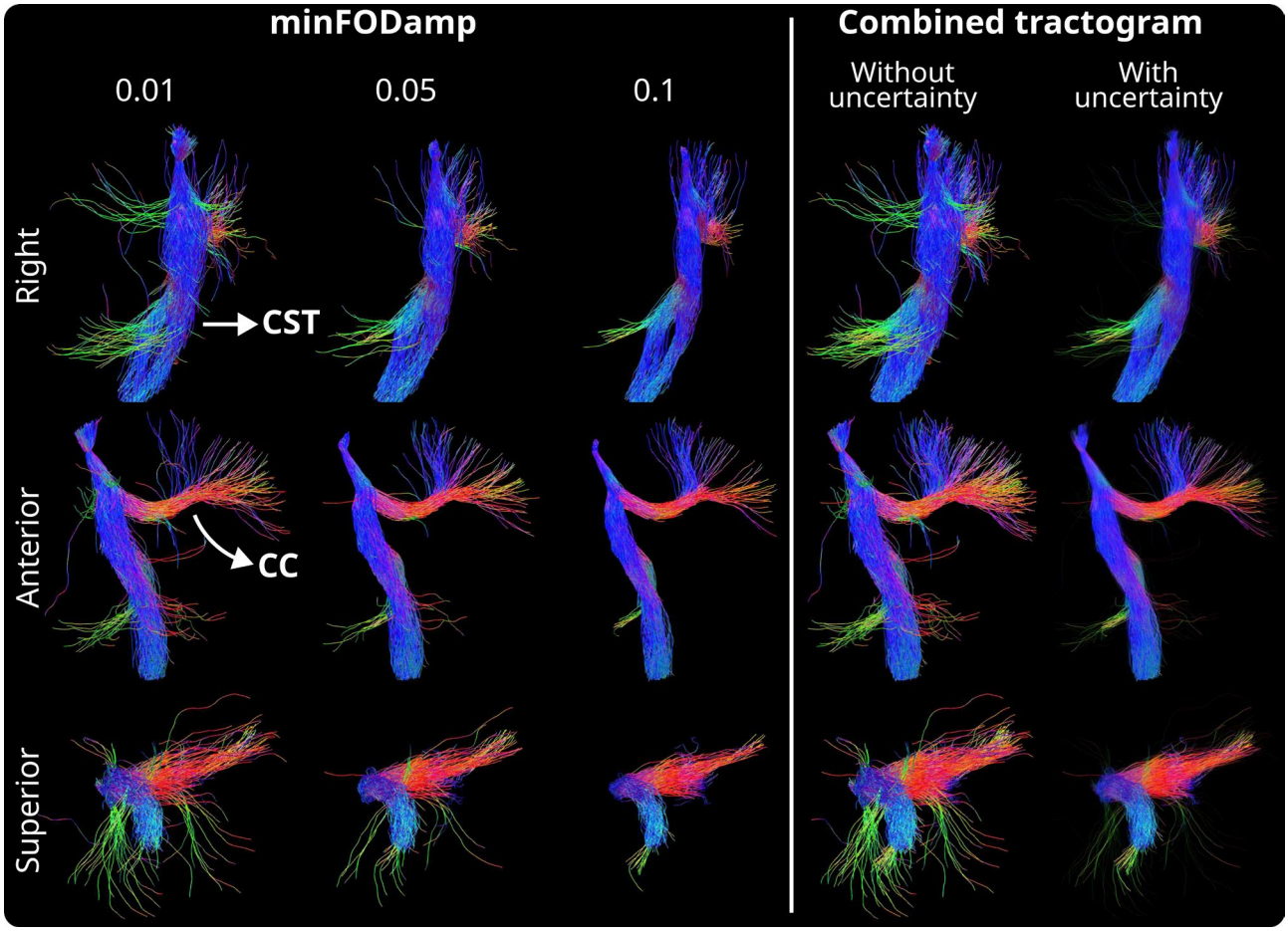

FIGURE 5 | Tractograms generated using a seed region placed on the motor cortex show cortico-spinal-tract (CST) and connections through the corpus callosum (CC), which are commonly studied in TMS experiments. The three rows show different views of the same tractogram. Tractograms show that increasing *minFODamp* produces streamlines that may not sample the whole extent of connections. Tractograms with lower *minFODamp* values reach more regions; however, streamlines lose organization, which can lead to increased false positives. Combination of the tractograms with uncertainty visualization shows all the streamlines. But because streamlines computed with lower *minFODamp* are shown with more transparency, user is provided with visual information that these connections are more likely to be false positives than other streamlines shown on display.

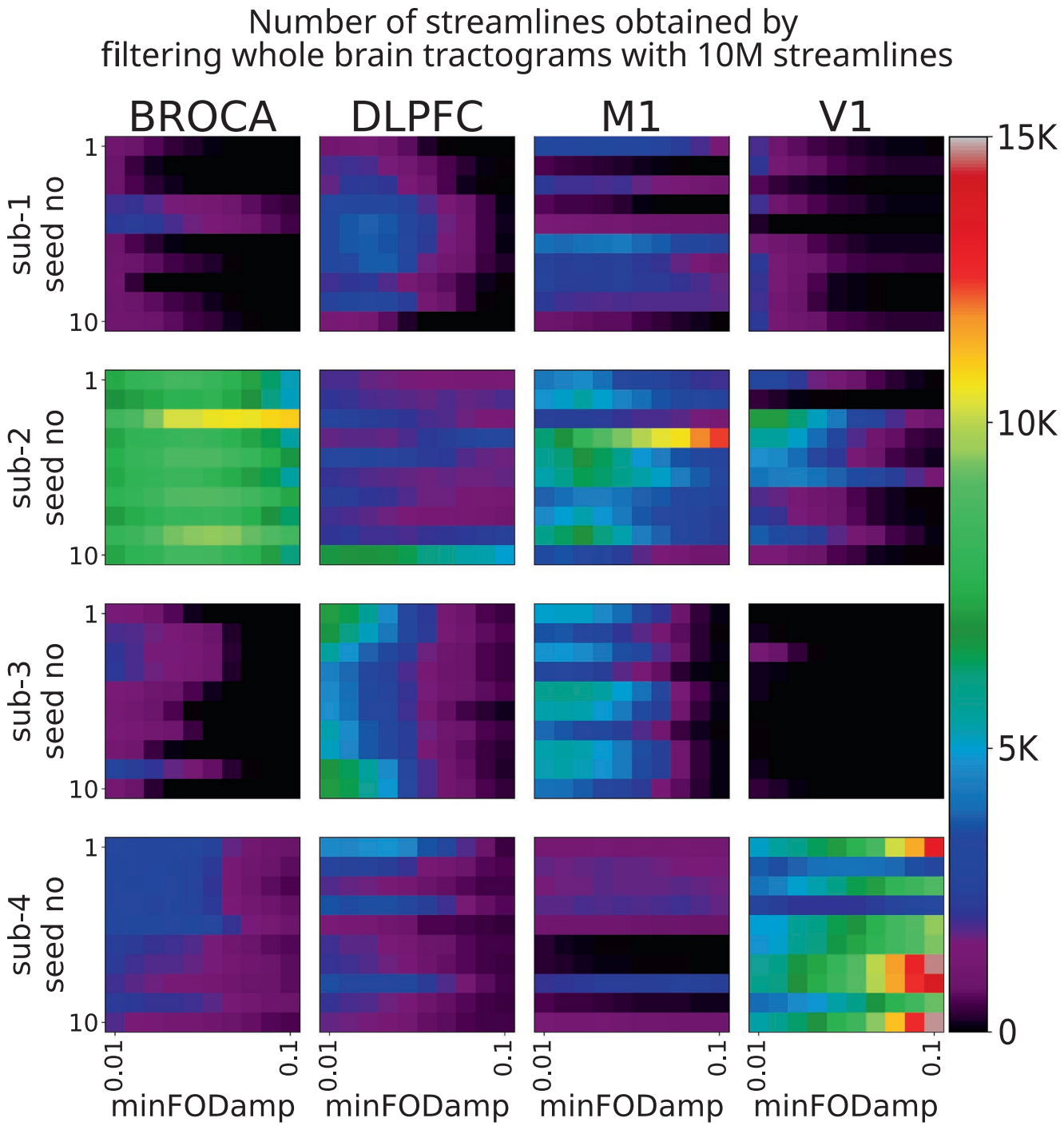

FIGURE 6 | The number of offline-filtered streamlines. Each value is obtained by selecting streamlines that pass through the seed regions from a whole-brain tractogram containing 10 million streamlines. Values are reported for each of the 10 repetitions of coil placement, that is, seed point, as well as 10 different *minFODamp* values.

Figure 7 shows overlap values for the seed-based approach used in real-time tractography-based neuronavigation. The overlap percentages for increasing number of streamlines were computed for each seed, against the corresponding reference tractogram with 1 million streamlines (see Section 3.2.3). As expected, the overlap increases with the number of streamlines. For comparison, we also computed the overlap between the results of the offline filtering approach and the reference tractograms. Black dots, "•," in Figure 7 show the closest overlap values obtained with the offline filtering results. The maximum number of dots, 64 out of 160 at 30000 streamlines, indicates that 40% of the seeds require 30,000 streamlines to be computed in real time to match the achievable overlap offline. There are 57 dots with arrows at 100000 streamlines, indicating that 35.6% of the seeds require at least 100,000 streamlines to match offline overlap levels. The remaining 24.4% of the seeds require less than 30,000 streamlines to be computed in real time to match the achievable offline

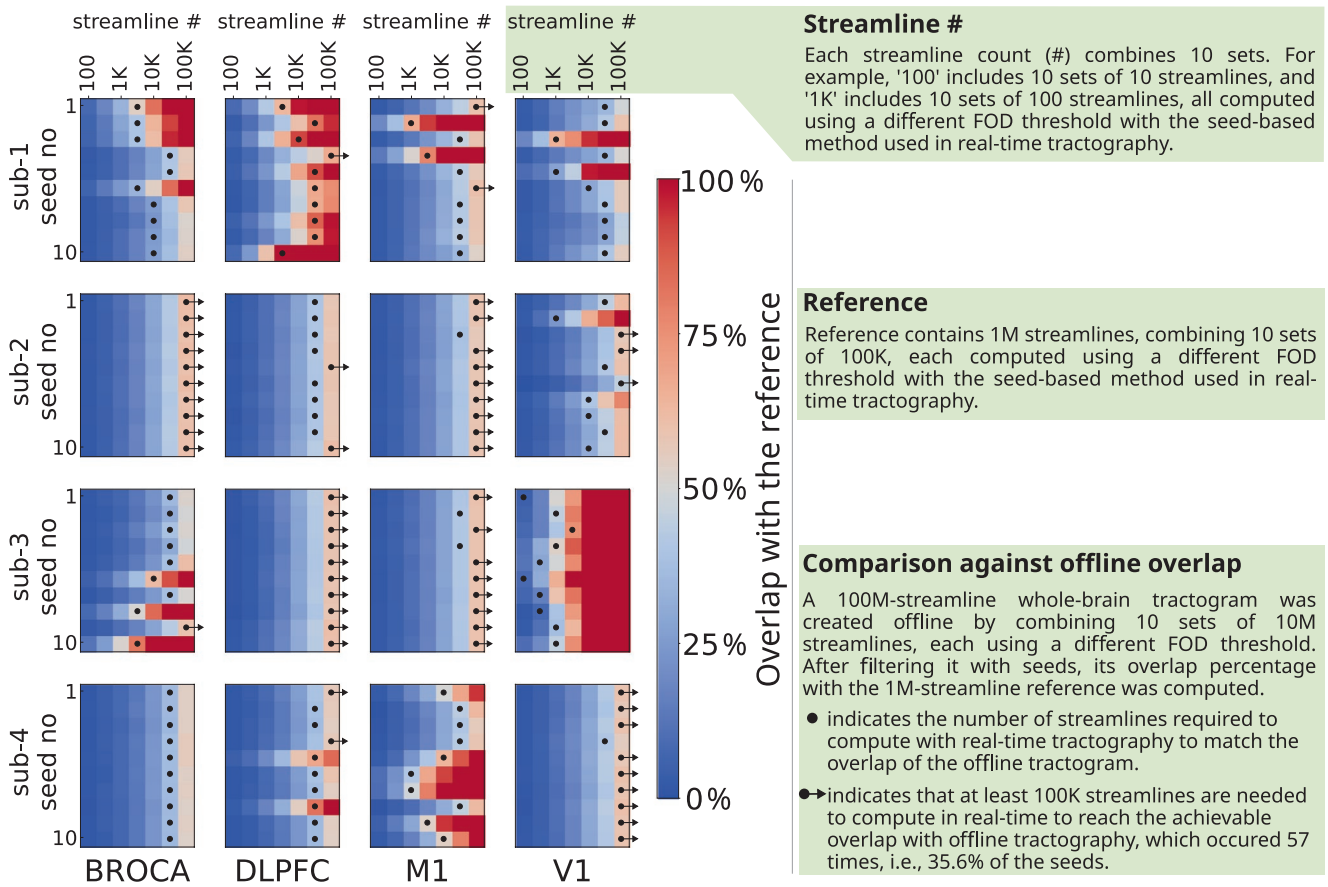

FIGURE 7 | Overlap percentages with respect to the number of streamlines. Here, the streamlines are obtained offline with the same method as the real-time case. The reference contains 1 million streamlines obtained by combining 10 seed-based tractograms (see Section 3.2.3). Each of the 10 tractograms are computed with a different *minFODamp* value and contains 100,000 streamlines. Black dots show the overlap obtained by filtering the whole-brain tractograms that contain 100 million streamlines for each seed.

overlap levels by the filtering approach. Seed-based tractography covers a large portion of the target area after a few thousands of streamlines—a few seconds in real-time operation. When compared to the filtering approach, seed-based tractography covers a larger portion of the brain after a few tens of thousands of streamlines for many seed points, for example, Broca's area of subject #1 or M1 of subject #4.

5 | Discussion

We developed a real-time platform for computing and visualizing brain's structural connections, specifically designed for guiding TMS applications. Our method uses state-of-the-art tractography practises that have received high scores in international challenges, providing highly accurate visual representations. These practises include: (i) a modern FOD computation method that can handle complex white-matter fiber organizations (Tran and Shi 2015), (ii) application of anatomical constraints (Smith et al. 2012), and (iii) a state-of-the-art fiber tracking algorithm (Aydogan and Shi 2021). These enhance tractogram quality over past real-time tools (Golby et al. 2011; Elhawary et al. 2011; Chamberland et al. 2014).

5.1 | Technical Aspects of Real-Time Tractography

Two methods to obtain streamlines for visualization in real-time include: (i) performing real-time fiber tracking, as we did, (ii) pre-computing many streamlines and selecting relevant ones in real time. The ability to adjust fiber tracking parameters is arguably the most important benefit of our system. Because even for the same brain, optimal tractography parameters vary depending on the region or the white-matter tract (Aydogan et al. 2018; Takemura et al. 2016), and fixing tractography parameters introduces biases across the brain (Girard et al. 2014). Real-time adjustment of parameters, which can be done through a simple user interface, is a key advantage when tracking fibers adjacent to tumors (Chamberland et al. 2014). On the other hand, the availability of a pre-computed whole-brain tractogram enables to compute connectivity strengths and matrices (Daducci et al. 2016)—not possible to compute with real-time seed-based tractography.

Tractography algorithms involve complexities beyond mere filtering of tractograms. However, real-time tractography has advantages when managing computer resources, because it does not require an interface between the hard drive and

memory. On the other hand, large pre-computed whole-brain tractograms (with 100 million streamlines), require a large disk space, which can introduce challenges in clinics when transferring data. While pre-filtering tractograms considering potential stimulation areas partly addresses this issue, it adds complexity, especially in cases like motor and speech mapping when pathology is involved. Additionally, it can pose challenges if pre-filtering assumptions require modification during the experiment. Alternatively, tractogram transmission techniques like TRAKO (Haehn et al. 2020) as well as strategies like saving only the endpoints or the coarse streamline skeletons could help the use of pre-computed tractograms in clinical settings. We should highlight that doing tractography in real time allows for flexible and on-the-fly exploration of brain connections, thereby bypassing the need for pre-determined stimulation areas. For instance, in a PAS experiment, where the requirement is to target the side opposite to the initial stimulation site, real-time tractography can be crucial in deciding the location for the coil.

Overall, both real-time tracking and filtering are suitable for tractography-assisted neuronavigation, and depending on the location in the brain, up to several hundreds or a few thousands streamlines per second can be obtained using standard computers. When compared against alternative offline practices, our real-time tractography pipeline does not compromise from quality to speed up the computation. Therefore, doing tractography in advance would not have improved the results that we show to the operator. Future research may lead to alternative visualization techniques that are capable of combining information from offline whole-brain tractograms, which has potential to enhance user experience and improve reproducibility, in addition to providing an option to highlight higher-order connections of the seed region and its connectivity strength with the rest of the brain.

5.2 | Design Aspects of Streamline Visualization and TMS Neuronavigation

Our work distinguishes from previous works through the use of novel visualization techniques: (i) Displaying tractograms with the peeled brain surface is a natural choice for TMS neuronavigation that was not demonstrated before. (ii) Our dynamic, incremental, visualization of streamlines, distributes the complicated connectivity information along time, helping the operator to interpret the complex information. In contrast to previous visualization approaches that show a snapshot for connectivity (Golby et al. 2011; Elhawary et al. 2011; Chamberland et al. 2014), we are showing a movie, where thousands of streamlines can be displayed in an iterative and sequential fashion. (iii) The uncertainty visualization approach is primarily designed for improved real-time experience, which to our knowledge, is the first time that transparency is used to convey information about uncertainty. While the exact overlap and overreach values shown in Figure 4 are going to be different for other data than the ISMRM 2015 challenge dataset, the performance trend is expected to be similar (Aydogan et al. 2018). As a result, our proposed uncertainty visualization provides a new view on the reliability of the streamlines. While we developed new methods for visualization and provided a qualitative evaluation, future research could answer whether the approaches quantitatively benefit the TMS application, for example, by improving treatment outcomes through individualized targeting.

5.3 | Impact of the Seeding Strategy

Our current setup estimates the seed region based on coil position and white-matter segmentation. The brain areas affected by TMS can be better estimated with the E-field distribution (Weise et al. 2020; Aberra et al. 2020; Sollmann et al. 2016). Even so, the response to TMS is still uncertain, and the fiber orientations can play a role (Laakso, Hirata, and Ugawa 2013). Because our approach does not account for E-field orientation (Souza et al. 2022), the output visualization should be interpreted accordingly. Notably, the transfer function in our work can be modified to reflect the interaction between the E-field and the visualized connections. Therefore, the integration of real-time E-field estimates and tractography might improve the accuracy of future TMS-targeting methods. Because TMS may primarily affect regions that are close to the coil (Siebner et al. 2022), gyral bias becomes a major problem for TMS neuronavigation with tractography. We believe this is reflected in the results shown in Figure 6. Even with a large number of streamlines (100 million), we observe that some regions were not reached by tractography, for example, V1 of subject #3. Starting with a whole-brain tractogram and selecting streamlines passing through a certain region results in a set of streamlines that follow various pathways, each supported by different FOD magnitudes. Depending on the underlying FOD data, the region may be connected with more streamlines supported by low FOD amplitudes or, conversely, more supported by high FOD amplitudes. This distribution is affected by various factors, including the region's connectivity to different parts of the brain, some of which are nearby and others more remote. Consequently, also depending on the other connections in the rest of the brain, altering the FOD threshold can increase, decrease, or maintain the number of connections associated with the region. In Figure 6, we not only observe poor streamline counts, but we also see a large variability for different subjects. For instance, while several thousands of streamlines could be obtained for most of the seeds in Broca's area of subject #2, no streamlines could be obtained for subject #1 and subject #3 for many seeds in the same region. Some of this variability may be due to differences in brain structure between individuals; however, we believe that the poor dMRI signal and fiber configuration variability around the cortex can be more significant factors. These highlight that even though we carefully adapted the state-of-the-art practices in our pipeline, there is room for improvement.

5.4 | Immediate Applications of Real-Time Tractography-Assisted TMS Neuronavigation

nTMS has been used with tractography to improve surgical outcomes (Picht et al. 2016) by identifying and visualizing eloquent motor areas during pre-operative planning (Frey et al. 2014). This is achieved by finding and saving nTMS-based seed points in a disk or hospital's picture archiving and communication system (PACS) (Mäkelä et al. 2015), followed by neurosurgeons using a separate software for seed-based tractography. Real-time

tractography-assisted TMS neuronavigation can save time and costs by eliminating the need for a separate tractography step. Furthermore, our system holds the potential to enhance existing neurosurgical workflows by offering detailed insights into brain connectivity. This is particularly important for targeted stimulation therapies aimed at treating neurological disorders like MDD (Riva-Posse et al. 2014). Additionally, our system can lead to innovations in surgical interventions since it enables the development of novel, personalized surgical strategies, which are tailored to the unique structural connectivity of each patient's brain (Shi et al. 2022; Eibl et al. 2024), as guided by functional measurements obtained through TMS. This capability not only has the potential to improve surgical precision but also to enhance treatment outcomes.

Our real-time tractography-assisted neuronavigation could be highly useful for PAS (Koch and Rothwell 2009; Koch et al. 2010). PAS has been shown to induce plastic changes (Classen et al. 2004), by involving stimulation of multiple targets, for example, two brain regions connected with cortico-cortical projections. Traditionally, one of the targets is set during the experiment based on functional measurements while the other targets are set manually based on anatomical MRI (Koch et al. 2013). For example, in Arai et al. (2012), a PAS experiment targeted the supplementary motor area (SMA) and M1. The M1 coil position was determined during the experiment based on electromyography (EMG) measurements in the first dorsal interosseous (FDI) muscle, while the SMA coil position relied on scalp-based measures. Similarly, Di Lorenzo et al. (2018) conducted a PAS experiment targeting M1 and the posterior parietal cortex (PPC), determining M1 placement during the experiment but using scalp-based positioning for PPC. Recently, Hernandez-Pavon et al. (2022) used dMRI-based tractography to post hoc demonstrate that their stimulation sites were connected. While coil positions for PAS can be determined prior to the experiment or using scalp-based measures, these paradigms often study effective connectivity between selected regions, with one target determined during the experiment. Real-time tractography-assisted neuronavigation enables more precise and personalized PAS protocols by identifying pairs that are structurally connected to each other during the experiment.

Recent developments in multi-channel TMS technology (Souza et al. 2022; Nieminen et al. 2022) opened a possibility for automated targeting (Tervo et al. 2022) and fast mapping of brain functions. Real-time tractography can play an important role for automated scanning algorithms to optimize stimulation parameters based on the underlying brain network. This would enable precise targeting of local and whole-brain networks for personalized connectomic neuromodulation (Horn and Fox 2020).

Our system currently does not record streamlines during real-time operation; however, we record the seed regions used to compute them, which can be used for post hoc analysis. The saved regions can be leveraged after the TMS measurement to investigate higher-order connections, study associated brain networks, or perform tractometric analyses to examine along-track properties (Yeatman et al. 2012). Additionally, post hoc analysis enables linking structural connections to TMS-induced responses, such as those measured with EMG, EEG, fMRI, or clinical and behavioral outcomes, helping the interpretation of TMS effects.

5.5 | Limitations

We believe tractography's limited accuracy, impacted by various factors, is the primary challenge for real-time tractography-assisted neuronavigation. dMRI data acquired with low resolution and/or few diffusion samples (Calabrese et al. 2014), and sub-optimal pre-processing choices could lead to low quality tractograms (Irfanoglu et al. 2012). Modern microstructure models, capable of distinguishing crossing fibers, have proven superior in tractography results compared to traditional techniques like DTI (Farquharson et al. 2013). The choice of tractography algorithms (Sarwar, Ramamohanarao, and Zalesky 2019), and the use of anatomical constraints were also shown to affect the results (Smith et al. 2012). Tractography is known to perform worse where fibers cross (Jeurissen et al. 2013). Moreover, the two-year long (2019–2020) IronTract challenge (https://irontract.mgh.harvard.edu/) showed that fiber configurations that go beyond crossing, for example, fanning, branching, can be more challenging for tractography (Maffei et al. 2020, 2022; Schilling et al. 2022). Due to differences in fiber configuration in gray and white matter, and the folded geometry of the brain, tractography algorithms also tend to be biased towards terminating the streamlines at gyral crowns (Reveley et al. 2015). Overall, tractograms contain large amounts of false positives and false negatives as has been shown in several previous validation studies and tractography competitions (Thomas et al. 2014; Maier-Hein et al. 2017; Schilling et al. 2019; Aydogan et al. 2018; Girard et al. 2020; Maffei et al. 2020, 2022). While the lack of standard protocols for image acquisition and other steps pose challenges for the translation of tractography-based techniques into clinics, there are ongoing efforts to establish consensus and standardization, for example, by the ISMRM Diffusion MRI Study Group. Despite the lack of widely accepted guidelines, there are resources that provide valuable insights such as the ConnectomeDB (Hodge et al. 2016). Moreover, advancements in MRI hardware and sequences can significantly enhance the quality of dMRI data. Techniques such as the HIBRID method (Fan et al. 2017) and the high-resolution protocol used in Nummenmaa et al. (2014) demonstrate the potential for improving the estimation of cortical fiber orientations and complex fiber configurations in the deep white matter.

In addition to the inherent limitations associated with tractography, our experiments were conducted with a small and homogeneous sample of four healthy male volunteers aged between 30 and 42, targeting four specific areas with TMS. Future studies should aim to include a more diverse and larger sample size and expand the set of targets to validate the broader applicability of real-time tractography-assisted neuronavigation. Another limitation concerns the specific parameters we used for dMRI acquisition, processing, and tractography, which influence the outcomes. Future studies would benefit from investigating the impact of these parameters on the results. By comparing our streamlines to the ISMRM 2015 tractography challenge results, we studied how the reconstructed connections in our study meet this key benchmark. Our evaluation on both synthetic and real

data was largely focused on quantitative measures, such as the number of streamlines and overlap percentages. However, this approach may overlook qualitative aspects, such as the clinical relevance of the visualized pathways and their interpretability by clinicians. We believe future experiments could benefit from a more comprehensive evaluation approach that incorporates qualitative feedback from TMS operators and neurosurgeons on the utility and user-friendliness of the system. Similarly, while we view the proposed uncertainty visualization in tractography as a significant advancement in conveying information about tractogram reliability, its practical impact on clinical decision-making and TMS neuronavigation was not within the scope of this study and remains underexplored. Further research is necessary to understand how uncertainty information is interpreted by practitioners in real-time scenarios and its influence on clinical outcomes.

In our study, we selected the region of interest in the brain for computing the tractography seeds without incorporating the TMS-induced E-field. Our ongoing efforts to integrate E-field estimates based on realistic head models into our neuronavigation system (Soto et al. 2023) are expected to provide more accurate structural connections likely affected by the TMS pulse.

Ensuring consistent targeting of the same connections with real-time tractography is critical for reliable TMS applications. Our previous work demonstrated a repeatability of less than 1 mm in translation and 1° in rotation for manual coil placement in our neuronavigation system (Souza et al. 2018). While the current study focuses on the feasibility of real-time tractography, a comprehensive evaluation of the repeatability of the obtained connections with larger, dedicated datasets, and its relationship to coil placement, remains an important direction for future work. Such consistent targeting of structural connections with high repeatability also requires precise seed localization relative to coil placement, which further emphasizes the inclusion of TMS-induced E-field estimations for determining seed regions.

While the aforementioned limitations impact the quality of tractography and our results, we believe that our techniques represent a significant progress in tractography-assisted neuronavigation, proposing a solution that shows the brain's anatomical connections in a way that is most accurate and helpful for brain stimulation, especially for TMS applications.

6 | Conclusion

We developed a real-time tractography-assisted neuronavigation system for TMS. To the best of our knowledge, the proposed system, distinguished by its unique features, is the first of its kind. Our neuronavigation software, InVesalius (https://invesalius.github.io/), which integrates our fiber tracking tool, Trekker (http://dmritrekker.github.io), are both open source projects hosted on GitHub. We anticipate that this technology is a critical step towards personalized brain stimulation targeting based on anatomical networks with potential applications in research and clinical environments.

Acknowledgments

This project has received funding from the Academy of Finland (grants #348631, #349985, and #353798), from Helsinki University Central Hospital (VTR grant #TYH2022224), and from the European Research Council (ERC) under the European Union's Horizon 2020 research and innovation programme (ConnectToBrain; grant agreement no. 810377). RHM has received funding from the Conselho Nacional de Desenvolvimento Científico e Tecnológico (grant no. 141056/2018-5) and from the FAPESP Research, Innovation and Dissemination Center for Neuromathematics (grant no. 2013/07699-0). Aalto NeuroImaging (ANI) infrastructure was used for MRI data collection at AMI, and for experiments at Aalto TMS. We thank Joonas Laurinoja and Tuomas Mutanen for their help with the video production. The authors acknowledge the computational resources provided by the Aalto Science-IT project.

Ethics Statement

Experiments were done after collecting written informed consents. The study was done in accordance with the Declaration of Helsinki and approved by the Coordinating Ethics Committee of the Hospital District of Helsinki and Uusimaa.

Conflicts of Interest

PL has been consulting Nexstim Plc in matters other than diffusion based navigated TMS. RJI has consulted Nexstim Plc and has several patents or patent applications related to TMS.

Data Availability Statement

The code and the ISMRM challenge data is publicly available. Data collected from the volunteers are available on request from the corresponding author with a data sharing agreement. Volunteer data are not publicly available due to privacy or ethical restrictions.

References

Aberra, A. S., B. Wang, W. M. Grill, and A. V. Peterchev. 2020. "Simulation of Transcranial Magnetic Stimulation in Head Model With Morphologically-Realistic Cortical Neurons." *Brain Stimulation* 13: 175–189. https://doi.org/10.1016/j.brs.2019.10.002.

Andersson, J. L. R., and S. N. Sotiropoulos. 2016. "An Integrated Approach to Correction for Off-Resonance Effects and Subject Movement in Diffusion MR Imaging." *NeuroImage* 125: 1063–1078. https://doi.org/10.1016/j.neuroimage.2015.10.019.

Arai, N., M. K. Lu, Y. Ugawa, and U. Ziemann. 2012. "Effective Connectivity Between Human Supplementary Motor Area and Primary Motor Cortex: A Paired-Coil TMS Study." *Experimental Brain Research* 220: 79–87.

Avants, B. B., N. Tustison, and G. Song. 2009. "Advanced Normalization Tools (ANTS)." *Insight Journal* 2: 1–35.

Aydogan, D. B. 2020. "Visualization of Uncertainty in Tractograms Using ROC-Based Transfer Functions for Real-Time TMS Applications." In *Proceedings of the 28th Annual Meeting of ISMRM*.

Aydogan, D. B., R. Jacobs, S. Dulawa, et al. 2018. "When Tractography Meets Tracer Injections: A Systematic Study of Trends and Variation Sources of Diffusion-Based Connectivity." *Brain Structure and Function* 223: 2841–2858. https://doi.org/10.1007/s00429-018-1663-8.

Aydogan, D. B., and Y. Shi. 2018. "Tracking and Validation Techniques for Topographically Organized Tractography." *NeuroImage* 181: 64–84. https://doi.org/10.1016/j.neuroimage.2018.06.071.

Aydogan, D. B., and Y. Shi. 2019. "A Novel Fiber-Tracking Algorithm Using Parallel Transport Frames." In *Proceedings of the 27th Annual Meeting of ISMRM*, Montreal.

Aydogan, D. B., and Y. Shi. 2021. "Parallel Transport Tractography." *IEEE Transactions on Medical Imaging* 40: 635–647. https://doi.org/10.1109/TMI.2020.3034038.

Bracht, T., D. Linden, and P. Keedwell. 2015. "A Review of White Matter Microstructure Alterations of Pathways of the Reward Circuit in Depression." *Journal of Affective Disorders* 187: 45–53.

Calabrese, E., A. Badea, C. L. Coe, G. R. Lubach, M. A. Styner, and G. A. Johnson. 2014. "Investigating the Tradeoffs Between Spatial Resolution and Diffusion Sampling for Brain Mapping With Diffusion Tractography: Time Well Spent?" *Human Brain Mapping* 35: 5667–5685.

Calamante, F., J. D. Tournier, G. D. Jackson, and A. Connelly. 2010. "Track-Density Imaging (TDI): Super-Resolution White Matter Imaging Using Whole-Brain Track-Density Mapping." *NeuroImage* 53: 1233–1243.

Cash, R. F., L. Cocchi, J. Lv, P. B. Fitzgerald, and A. Zalesky. 2021. "Functional Magnetic Resonance Imaging–Guided Personalization of Transcranial Magnetic Stimulation Treatment for Depression." *JAMA Psychiatry* 78: 337–339. https://doi.org/10.1001/jamapsychiatry580.2020.3794.

Chamberland, M., K. Whittingstall, D. Fortin, D. Mathieu, and M. Descoteaux. 2014. "Real-Time Multi-Peak Tractography for Instantaneous Connectivity Display." *Frontiers in Neuroinformatics* 8: 59.

Chen, D. Q., F. Dell'Acqua, A. Rokem, et al. 2019. "Diffusion Weighted Image Co-Registration: Investigation of Best Practices." BioRxiv, 864108.

Classen, J., A. Wolters, K. Stefan, et al. 2004. "Paired Associative Stimulation." *Supplements to Clinical Neurophysiology* 57: 563–569.

Corina, D. P., B. C. Loudermilk, L. Detwiler, R. F. Martin, J. F. Brinkley, and G. Ojemann. 2010. "Analysis of Naming Errors During Cortical Stimulation Mapping: Implications for Models of Language Representation." *Brain and Language* 115: 101–112.

Daducci, A., A. Dal Palú, M. Descoteaux, and J. P. Thiran. 2016. "Microstructure Informed Tractography: Pitfalls and Open Challenges." *Frontiers in Neuroscience* 10: 247.

Dannhauer, M., L. J. Gomez, P. L. Robins, et al. 2024. "Electric Field Modeling in Personalizing TMS Interventions." *Biological Psychiatry* 95, no. 6: 494–501.

Di Lazzaro, V., and J. C. Rothwell. 2014. "Corticospinal Activity Evoked and Modulated by Non-Invasive Stimulation of the Intact Human Motor Cortex." *Journal of Physiology* 592: 4115–4128. https://doi.org/10.1113/jphysiol.2014.274316.

Di Lorenzo, F., V. Ponzo, C. Motta, et al. 2018. "Impaired Spike Timing Dependent Cortico-Cortical Plasticity in Alzheimer's Disease Patients." *Journal of Alzheimer's Disease* 66: 983–991.

Eibl, T., M. Schrey, A. Liebert, et al. 2024. "Significance of Navigated Transcranial Magnetic Stimulation and Tractography to Preserve Motor Function in Patients Undergoing Surgery for Motor Eloquent Gliomas." *Heliyon* 10: e28115.

Elhawary, H., H. Liu, P. Patel, et al. 2011. "Intraoperative Real-Time Querying of White Matter Tracts During Frameless Stereotactic Neuronavigation." *Neurosurgery* 68: 506–516.

Fan, Q., A. Nummenmaa, J. R. Polimeni, et al. 2017. "High b-Value and High Resolution Integrated Diffusion (HIBRID) Imaging." *NeuroImage* 150: 162–176.

Farquharson, S., J. D. Tournier, F. Calamante, et al. 2013. "White Matter Fiber Tractography: Why We Need to Move Beyond DTI." *Journal of Neurosurgery* 118: 1367–1377.

Fischl, B. 2012. "Freesurfer." *NeuroImage* 62: 774–781.

Fitzgerald, P. B., K. Hoy, S. McQueen, et al. 2009. "A Randomized Trial of rTMS Targeted With MRI Based Neuro-Navigation in Treatment-Resistant Depression." *Neuropsychopharmacology* 34: 1255–1262.

Frey, D., S. Schilt, V. Strack, et al. 2014. "Navigated Transcranial Magnetic Stimulation Improves the Treatment Outcome in Patients With Brain Tumors in Motor Eloquent Locations." *Neuro-Oncology* 16: 1365–1372.

Garyfallidis, E., M. Brett, B. Amirbekian, et al. 2014. "Dipy, a Library for the Analysis of Diffusion MRI Data." *Frontiers in Neuroinformatics* 8: 8. https://doi.org/10.3389/fninf.2014.00008.

Girard, G., R. Caminiti, A. Battaglia-Mayer, et al. 2020. "On the Cortical Connectivity in the Macaque Brain: A Comparison of Diffusion Tractography and Histological Tracing Data." *NeuroImage* 221: 117201.

Girard, G., K. Whittingstall, R. Deriche, and M. Descoteaux. 2014. "Towards Quantitative Connectivity Analysis: Reducing Tractography Biases." *NeuroImage* 98: 266–278.

Golby, A. J., G. Kindlmann, I. Norton, A. Yarmarkovich, S. Pieper, and R. Kikinis. 2011. "Interactive Diffusion Tensor Tractography Visualization for Neurosurgical Planning." *Neurosurgery* 68: 496–505.

Grosprêtre, S., C. Ruffino, and F. Lebon. 2016. "Motor Imagery and Cortico-Spinal Excitability: A Review." *European Journal of Sport Science* 16: 317–324.

Haehn, D., L. Franke, F. Zhang, et al. 2020. "TRAKO: Efficient Transmission of Tractography Data for Visualization." In *Medical Image Computing and Computer Assisted Intervention–MICCAI 2020: 23rd International Conference, Lima, Peru, October 4–8, 2020, Proceedings, Part VII*, 322–332. Springer-Verlag, Berlin, Heidelberg: Springer.

Hannula, H., and R. J. Ilmoniemi. 2017. *Basic Principles of Navigated TMS*, 3–29. Cham: Springer International Publishing. https://doi.org/10.1007/978-3-319-54918-7_1.

Hernandez-Pavon, J. C., N. Schneider-Garces, J. P. Begnoche, L. E. Miller, and T. Raij. 2022. "Targeted Modulation of Human Brain Interregional Effective Connectivity With Spike-Timing Dependent Plasticity." *Neuromodulation: Technology at the Neural Interface* 26: 745–754. https://doi.org/10.1016/j.neurom.2022.10.045.

Hodge, M. R., W. Horton, T. Brown, et al. 2016. "Connectomedb—Sharing Human Brain Connectivity Data." *NeuroImage* 124: 1102–1107.

Horn, A., and M. D. Fox. 2020. "Opportunities of Connectomic Neuromodulation." *NeuroImage* 221: 117180. https://doi.org/10.1016/j.neuroimage.2020.117180.

Irfanoglu, M. O., L. Walker, J. Sarlls, S. Marenco, and C. Pierpaoli. 2012. "Effects of Image Distortions Originating From Susceptibility Variations and Concomitant Fields on Diffusion MRI Tractography Results." *NeuroImage* 61: 275–288.

Jeurissen, B., A. Leemans, J. D. Tournier, D. K. Jones, and J. Sijbers. 2013. "Investigating the Prevalence of Complex Fiber Configurations in White Matter Tissue With Diffusion Magnetic Resonance Imaging." *Human Brain Mapping* 34: 2747–2766.

Koch, G., M. Cercignani, C. Pecchioli, et al. 2010. "In Vivo Definition of Parieto-Motor Connections Involved in Planning of Grasping Movements." *NeuroImage* 51: 300–312.

Koch, G., V. Ponzo, F. Di Lorenzo, C. Caltagirone, and D. Veniero. 2013. "Hebbian and Anti-Hebbian Spike-Timing-Dependent Plasticity of Human Cortico-Cortical Connections." *Journal of Neuroscience* 33: 9725–9733.

Koch, G., and J. C. Rothwell. 2009. "TMS Investigations Into the Task-Dependent Functional Interplay Between Human Posterior Parietal and Motor Cortex." *Behavioural Brain Research* 202: 147–152.

Korgaonkar, M. S., A. Fornito, L. M. Williams, and S. M. Grieve. 2014. "Abnormal Structural Networks Characterize Major Depressive Disorder: A Connectome Analysis." *Biological Psychiatry* 76: 567–574.

Korgaonkar, M. S., S. M. Grieve, S. H. Koslow, J. D. Gabrieli, E. Gordon, and L. M. Williams. 2011. "Loss of White Matter Integrity in Major Depressive Disorder: Evidence Using Tract-Based Spatial Statistical Analysis of Diffusion Tensor Imaging." *Human Brain Mapping* 32: 2161–2171.

Krieg, S. M., P. Lioumis, J. P. Mäkelä, et al. 2017. "Protocol for Motor and Language Mapping by Navigated TMS in Patients and Healthy Volunteers; Workshop Report." *Acta Neurochirurgica* 159: 1187–1195.

Laakso, I., A. Hirata, and Y. Ugawa. 2013. "Effects of Coil Orientation on the Electric Field Induced by TMS Over the Hand Motor Area." *Physics in Medicine & Biology* 59: 203–218.

Lefaucheur, J. P., N. André-Obadia, A. Antal, et al. 2014. "Evidence-Based Guidelines on the Therapeutic Use of Repetitive Transcranial Magnetic Stimulation (rTMS)." *Clinical Neurophysiology* 125: 2150–2206.

Lefaucheur, J. P., and T. Picht. 2016. "The Value of Preoperative Functional Cortical Mapping Using Navigated TMS." *Neurophysiologie Clinique/Clinical Neurophysiology* 46: 125–133.

Lioumis, P., S. Autti, J. Wilenius, et al. 2023. "Study Design for Navigated Repetitive Transcranial Magnetic Stimulation for Speech Cortical Mapping." *JoVE (Journal of Visualized Experiments)* 2023, no. 193: 1–14.

Lioumis, P., D. Kičić, P. Savolainen, J. P. Mäkelä, and S. Kähkönen. 2009. "Reproducibility of TMS-Evoked EEG Responses." *Human Brain Mapping* 30: 1387–1396.

Lioumis, P., A. Zhdanov, N. Mäkelä, et al. 2012. "A Novel Approach for Documenting Naming Errors Induced by Navigated Transcranial Magnetic Stimulation." *Journal of Neuroscience Methods* 204: 349–354.

Llufriu, S., E. Martinez-Heras, E. Solana, et al. 2017. "Structural Networks Involved in Attention and Executive Functions in Multiple Sclerosis." *NeuroImage: Clinical* 13: 288–296. https://doi.org/10.1016/j.nicl.2016.11.026.

Lo, C. Y., P. N. Wang, K. H. Chou, J. Wang, Y. He, and C. P. Lin. 2010. "Diffusion Tensor Tractography Reveals Abnormal Topological Organization in Structural Cortical Networks in Alzheimer's Disease." *Journal of Neuroscience* 30: 16876–16885.

Maffei, C., G. Girard, K. G. Schilling, et al. 2020. "The IronTract Challenge: Validation and Optimal Tractography Methods for the HCP Diffusion Acquisition Scheme." In *ISMRM, Virtual*.

Maffei, C., G. Girard, K. G. Schilling, et al. 2022. "Insights From the IronTract Challenge: Optimal Methods for Mapping Brain Pathways From Multi-Shell Diffusion MRI." *NeuroImage* 257: 119327.

Maier-Hein, K. H., P. F. Neher, J. C. Houde, et al. 2017. "The Challenge of Mapping the Human Connectome Based on Diffusion Tractography." *Nature Communications* 8: 1–13. https://doi.org/10.1038/s41467-017-01285-x.

Mäkelä, T., A. M. Vitikainen, A. Laakso, and J. P. Mäkelä. 2015. "Integrating nTMS Data Into a Radiology Picture Archiving System." *Journal of Digital Imaging* 28: 428–432. https://doi.org/10.1007/s10278-015-9768-6.

Nath, V., K. G. Schilling, P. Parvathaneni, et al. 2020. "Tractography Reproducibility Challenge With Empirical Data (TraCED): The 2017 ISMRM Diffusion Study Group Challenge." *Journal of Magnetic Resonance Imaging* 51: 234–249.

Nieminen, J. O., H. Sinisalo, V. H. Souza, et al. 2022. "Multi-Locus Transcranial Magnetic Stimulation System for Electronically Targeted Brain Stimulation." *Brain Stimulation* 15: 116–124. https://doi.org/10.1016/j.brs.2021.11.014.

Nummenmaa, A., J. A. McNab, P. Savadjiev, et al. 2014. "Targeting of White Matter Tracts With Transcranial Magnetic Stimulation." *Brain Stimulation* 7: 80–84.

Pelissolo, A., G. Harika-Germaneau, F. Rachid, et al. 2016. "Repetitive Transcranial Magnetic Stimulation to Supplementary Motor Area in Refractory Obsessive-Compulsive Disorder Treatment: A Sham-Controlled Trial." *International Journal of Neuropsychopharmacology* 19: pyw025.

Picht, T., D. Frey, S. Thieme, S. Kliesch, and P. Vajkoczy. 2016. "Presurgical Navigated TMS Motor Cortex Mapping Improves Outcome in Glioblastoma Surgery: A Controlled Observational Study." *Journal of Neuro-Oncology* 126: 535–543. https://doi.org/10.1007/s11060-015-1993-9.

Reveley, C., A. K. Seth, C. Pierpaoli, et al. 2015. "Superficial White Matter Fiber Systems Impede Detection of Long-Range Cortical Connections in Diffusion MR Tractography." *Proceedings of the National Academy of Sciences* 112: E2820–E2828.

Riva-Posse, P., K. S. Choi, P. E. Holtzheimer, et al. 2014. "Defining Critical White Matter Pathways Mediating Successful Subcallosal Cingulate Deep Brain Stimulation for Treatment-Resistant Depression." *Biological Psychiatry* 76: 963–969.

Rubinov, M., and O. Sporns. 2010. "Complex Network Measures of Brain Connectivity: Uses and Interpretations." *NeuroImage* 52: 1059–1069.

Ruohonen, J., and J. Karhu. 2010. "Navigated Transcranial Magnetic Stimulation." *Clinical Neurophysiology* 40: 7–17.

Sarwar, T., K. Ramamohanarao, and A. Zalesky. 2019. "Mapping Connectomes With Diffusion MRI: Deterministic or Probabilistic Tractography?" *Magnetic Resonance in Medicine* 81: 1368–1384.

Schilling, K. G., V. Nath, C. Hansen, et al. 2019. "Limits to Anatomical Accuracy of Diffusion Tractography Using Modern Approaches." *NeuroImage* 185: 1–11. https://doi.org/10.1016/j.neuroimage.2018.10.029.

Schilling, K. G., F. Rheault, L. Petit, et al. 2021. "Tractography Dissection Variability: What Happens When 42 Groups Dissect 14 White Matter Bundles on the Same Dataset?" *NeuroImage* 243: 118502.

Schilling, K. G., C. M. Tax, F. Rheault, et al. 2022. "Prevalence of White Matter Pathways Coming Into a Single White Matter Voxel Orientation: The Bottleneck Issue in Tractography." *Human Brain Mapping* 43: 1196–1213.

Shi, J., D. Lu, R. Pan, et al. 2022. "Applications of Diffusion Tensor Imaging Integrated With Neuronavigation to Prevent Visual Damage During Tumor Resection in the Optic Radiation Area." *Frontiers in Oncology* 12: 955418.

Shi, Y., and A. Toga. 2017. "Connectome Imaging for Mapping Human Brain Pathways." *Molecular Psychiatry* 22: 1230–1240.

Siebner, H. R., K. Funke, A. S. Aberra, et al. 2022. "Transcranial Magnetic Stimulation of the Brain: What Is Stimulated?–A Consensus and Critical Position Paper." *Clinical Neurophysiology* 140: 59–97.

Smith, R. E., J. D. Tournier, F. Calamante, and A. Connelly. 2012. "Anatomically-Constrained Tractography: Improved Diffusion MRI Streamlines Tractography Through Effective Use of Anatomical Information." *NeuroImage* 62: 1924–1938.

Sollmann, N., M. F. Goblirsch-Kolb, S. Ille, et al. 2016. "Comparison Between Electric-Field-Navigated and Line-Navigated TMS for Cortical Motor Mapping in Patients With Brain Tumors." *Acta Neurochirurgica* 158: 2277–2289.

Sollmann, N., H. Zhang, A. Fratini, et al. 2020. "Risk Assessment by Presurgical Tractography Using Navigated TMS Maps in Patients With Highly Motor-or Language-Eloquent Brain Tumors." *Cancers* 12: 1264.

Soto, A. M., V. H. Souza, R. H. Matsuda, et al. 2023. "Real-Time e-Field Neuronavigation for Transcranial Magnetic Stimulation." *Brain Stimulation: Basic, Translational, and Clinical Research in Neuromodulation* 16: 363.

Souza, V. H., R. H. Matsuda, A. S. Peres, et al. 2018. "Development and Characterization of the InVesalius Navigator Software for Navigated Transcranial Magnetic Stimulation." *Journal of Neuroscience Methods* 309: 109–120.

Souza, V. H., J. O. Nieminen, S. Tugin, L. M. Koponen, O. Baffa, and R. J. Ilmoniemi. 2022. "TMS With Fast and Accurate Electronic Control: Measuring the Orientation Sensitivity of Corticomotor Pathways." *Brain Stimulation* 15: 306–315. https://doi.org/10.1016/j.brs.2022.01.009.

Takemura, H., C. F. Caiafa, B. A. Wandell, and F. Pestilli. 2016. "Ensemble Tractography." *PLoS Computational Biology* 12: e1004692.

Terao, Y., and Y. Ugawa. 2002. "Basic Mechanisms of TMS." *Journal of Clinical Neurophysiology* 19: 322–343.

Tervo, A. E., J. O. Nieminen, P. Lioumis, et al. 2022. "Closed-Loop Optimization of Transcranial Magnetic Stimulation With Electroencephalography Feedback." *Brain Stimulation* 15: 523–531. https://doi.org/10.1016/j.brs.2022.01.016.

Thomas, C., F. Q. Ye, M. O. Irfanoglu, et al. 2014. "Anatomical Accuracy of Brain Connections Derived From Diffusion MRI Tractography Is Inherently Limited." *Proceedings of the National Academy of Sciences* 111: 16574–16579.

Tran, G., and Y. Shi. 2015. "Fiber Orientation and Compartment Parameter Estimation From Multi-Shell Diffusion Imaging." *IEEE Transactions on Medical Imaging* 34: 2320–2332.

Tremblay, S., N. C. Rogasch, I. Premoli, et al. 2019. "Clinical Utility and Prospective of TMS-EEG." *Clinical Neurophysiology* 130: 802–844.

Van Essen, D. C. 2013. "Cartography and Connectomes." *Neuron* 80: 775–790. https://doi.org/10.1016/j.neuron.2013.10.027.

Veraart, J., D. S. Novikov, D. Christiaens, B. Ades-aron, J. Sijbers, and E. Fieremans. 2016. "Denoising of Diffusion MRI Using Random Matrix Theory." *NeuroImage* 142: 394–406. https://doi.org/10.1016/j.neuroimage.2016.08.016.

Voineskos, A. N., F. Farzan, M. S. Barr, et al. 2010. "The Role of the Corpus Callosum in Transcranial Magnetic Stimulation Induced Interhemispheric Signal Propagation." *Biological Psychiatry* 68: 825–831.

Wandell, B. A. 2016. "Clarifying Human White Matter." *Annual Review of Neuroscience* 39: 103–128.

Weise, K., O. Numssen, A. Thielscher, G. Hartwigsen, and T. R. Knösche. 2020. "A Novel Approach to Localize Cortical TMS Effects." *NeuroImage* 209: 116486. https://doi.org/10.1016/j.neuroimage.2019.116486.

Yamada, K., H. Ito, H. Nakamura, et al. 2004. "Stroke Patients' Evolving Symptoms Assessed by Tractography." *Journal of Magnetic Resonance Imaging* 20: 923–929. https://doi.org/10.1002/jmri.20215.

Yeatman, J. D., R. F. Dougherty, N. J. Myall, B. A. Wandell, and H. M. Feldman. 2012. "Tract Profiles of White Matter Properties: Automating Fiber-Tract Quantification." *PLoS One* 7: e49790.

Yendiki, A., M. Aggarwal, M. Axer, A. F. Howard, A. M. van Cappellen van Walsum, and S. N. Haber. 2022. "Post Mortem Mapping of Connectional Anatomy for the Validation of Diffusion MRI." *NeuroImage* 256: 119146. https://doi.org/10.1016/j.neuroimage.2022.119146.

Supporting Information

Additional supporting information can be found online in the Supporting Information section.